Transportation Networks Optimized for Various Income Groups and their Impact on the Spread of Airborne Disease

Jaysha Camacho[1], Rachel Matheson[2], Juliana Noguera[3], Brandon Summers[4], Nanda Mallapragada[5], and Dr. Baojun Song[6]

The Mathematical and Theoretical Biology Institute, Tempe, Arizona

[1] *University of Florida, Gainesville, Florida*

[2] *Vassar College, Poughkeepsie, New York*

[3] *Los Andes University, Bogotá D.C., Colombia*

[4] *North Carolina State University, Raleigh, North Carolina*

[5] *Arizona State University, Tempe, Arizona*

[6] *Montclair State University, Montclair, New Jersey*

Abstract

With growing reliance on mass transit systems in American cities, the question of access becomes more important. This study aims to explore the spread of an infectious disease across a transportation network created to optimize access to most frequented destinations for distinct socioeconomic groups. First, we develop a theoretical model of a city, based on the Kohl model for urban growth which assumes distinct regions where income groups live and work. It is assumed that all income groups in this city are transit-dependent. In this framework, we maximize "satisfaction," a measure of how easily the population of a neighborhood can travel to desirable destinations, through placement of bus routes. Within this framework we connect a single-outbreak multi-patch SIR model of Influenza A, incorporating the effects of attraction and travel time into the incidence rate. We track the populations' interactions through contact within their neighborhoods, within the transit network, and with other transit-connected neighborhoods. We observe how the basic reproductive number is affected by the layout of the optimized transportation network. Results show that use of public transportation largely does not affect the global epidemic but that more equal time spent in transit leads to less disparate patch-specific epidemic outcomes.

1 Introduction

Many American cities are currently undergoing demographic inversion. Demographic inversion refers to the trend of suburbs of a city becoming the principal region where immigrants and minorities settle due to the continuous increase in cost of living in central city areas [1]. For example, Atlanta has historically been home to a majority black community, but between 2000 and 2010, the percentage of African-American residents within the city fell from 61% to 54%, while in the same time period, suburban counties like Clayton and DeKalb saw an increase in black population. Washington, D.C. is undergoing a similar inversion [2]. From 2000 to 2008-2012, the percentage of suburban poor in America increased by 139%, which is nearly three times more than within cities. By 2008-2012, 46% of all non-rural poor residents living in concentrated poverty lived in the suburbs [3]. Large metropolitan suburbs house about one-third of low-income Americans, a greater share than big cities, small metropolitan areas, or rural areas. Through the 2000s, suburban poverty increased at a rate five times more to what we have seen within cities [4].

On the other hand, over the last 20 years, American transit ridership has increased by 32%, creating a need for more robust transit systems [5, 6]. There are many advantages to high-quality transit services, including equity benefits for disadvantaged users [7]. Studies have shown that the primary reason for central city poverty is access to the public transportation system [8]. Upward mobility, that is the capacity of increasing one's social or economic position, is currently higher in cities with less sprawl, as measured by commute times to work [9, 10]. This suggests that job access, economic segregation, and transportation access are strongly correlated and interdependent. However, transit extensions may not be designed to fully serve disadvantaged users.

Urban economics literature has developed different types of models to analyze the socioeconomic distribution of a city. One of the most well-known monocentric city models, created by Ernest W. Burgess in 1925 [11], posits that the large American city can be generalized to have a central business district surrounded by a zone of transition including other industries, followed by inner-city poor residences and then high-income residences located in the suburbs. This is contextualized within an industrial city, where the wealthy prefer the suburbs because of pollution and violence downtown, while lower-income people prioritize lower transit costs. This model is still in use today but is seen as outdated as the post-industrial processes of gentrification and displacement become increasingly more common. An older monocentric city model was created in 1841 by J.G. Kohl [11], based on the pre-industrial cities of continental Europe, in which the high-income population was housed in the city center and the low-income communities resided farther from the city. At this time, transit costs were very high so the wealthy preferred to live downtown near the destinations they desired most [12]. With demographic inversion occurring in many large American cities, the Kohl model becomes relevant again in such cases.

This layout mirrors the makeup of New York City, one the few cities that underwent demographic inversion in the 1970s. In 2007, new households in the Financial District had a median income of $256,000 and were 74% single adults or childless couples [2]. In New York City, wealthy Manhattan is located at the center of the city whereas Queens, the Bronx, and Brooklyn with less concentrated wealth and more concentrated poverty are farther from the center. Taking a close look at a map of the New York City subway reveals the fact that there is considerably more transit access in the central city than in Queens or in the Bronx, showing that the system has been designed to serve the wealthy communities better than the poor [8].

Moreover, the current work in transportation modeling is based on the principle of demand and cost-benefit analysis. As a result, their work reproduces already imbalanced transit provisions, ignoring populations that do not already have transportation access. Martens suggest changing the base of the model to the principle of need in order to have a minimal level of transport service for the entire population [13]. An interesting question arises when we consider the socioeconomic reverberations of the placement of public transit infrastructure: What does an "equitable" transit system look like? Furthermore, we may ask how it compares to a network optimized for the wealthy or for both.

When the people are more connected, the potential to create devastating epidemics increases. Public transportation creates an ideal environment for disease spread: Each bus creates an environment where a high concentration of dust particles or water droplets allow biological agents to float in the air, at temperatures that favor their rapid growth.[14, 15]. Most of the airborne diseases are caused by different pathogens such as viruses, bacteria, and fungus that are released into the air by normal processes such as sneezing, coughing and laughing [15, 16]. The hard surfaces of buses and trains provide an ideal environment for viruses to spread as they extend the survival time of viruses, unlike porous surfaces [17].

Even if transportation networks were developed to serve the low- and high-income groups equitably, what public health consequences would stem from improved transportation access? How does varying public transportation infrastructure affect the spread of disease in a city? We aim to investigate these questions by looking at how influenza, a common infectious disease, can spread through a theoretical city under different optimized public transit arrangements.

Influenza can spread through direct contact between individuals, indirect contact with contaminated objects, droplet transmission, or airborne transmission through infectious droplet nuclei that can linger in the air. Airborne transmission can only be dealt with through air-handling and ventilation procedures [18, 19]. For example, public health researchers at the University of Nottingham found that recent bus or train use within 5 days of influenza symptoms is associated with six times higher risk of a doctor visit for an acute respiratory infection [20]. Another study on tuberculosis in

South Africa found that, although the average number of passengers sharing an indoor space was higher in trains than in minibus taxis, minibus taxi commuters faced a higher risk of tuberculosis infection, which they attributed to poor ventilation and high respiratory contact rates within the minibus taxis [21]. As well, health facilities with many infectious patients experience higher risks of infectious disease transmission when paired with poor ventilation infrastructure [22].This showcases the importance of ventilation in slowing the spread of airborne disease. Another tuberculosis study was focused on transmission within school buses in Houston, Texas. They found that higher rates of transmission coincided with duration of the bus ride [23], signaling that the longer the time spent by an individual in the enclosed environment, the more prone he or she is to the contagion.

In developing better transit infrastructure, we are concerned in particular about the impact on the health of disadvantaged users. The World Health Organization (WHO) identified poverty as a major contributor to vulnerability, or the level to which a population can resist environmental health disasters, including disease outbreaks [22]. Thus, we wish to focus on the health outcomes of people by economic class.

Past work has been done on the spread of influenza in a city, mainly relying on simulations [12, 16]. We focus on the impact of public transportation on specific income groups in urban cities capturing the Kohl model of income distribution. Different income groups have varied preferences for different destinations. We build upon former work by Song and Castillo-Chavez [24] on virtual mass transportation by adapting their model to consider a population of solely bus riders who interact in a proportional mixing scheme within the public transportation network as well as within transit-connected neighborhoods, placing it on top of our theoretical transportation model. Between our theoretical and epidemic model we will be able to picture how public transportation facilitates the spread of airborne disease in various neighborhoods.

Our paper will investigate Influenza A (H3N2) as it is currently one of the most prevalent strains of influenza: In 2016-2017, 75% of all positive influenza tests were A (H3N2) [25]. We then explore how the basic reproductive number is affected by our transportation networks, by employing sensitivity analysis. We also place our epidemiological model on top of our theoretical model and run it as a simulation. Results show that public transportation largely does not affect the global epidemic but that more equal time spent in transit leads to less disparate epidemic outcomes.

2 Methods and Model Description

Two models are developed and linked in order to understand how transportation systems in an urban city can affect the spread of airborne disease. The first model is a type of lattice grid, used to find the optimal location of bus routes for various income groups in a theoretical city. The second is an epidemic SIR model that describes the spread of influenza in an urban city with optimized bus transportation systems (generated from first model).

2.1 Transportation Network Model

First, we assume that all city residents are transit-dependent (can only either walk or take the bus). Second, we contextualize our transportation network in an already-existing city layout. To create the city layout we use a variation of the Kohl model (Figure 1a). This variation is based on bid-rent theory[1] leading to the development of the classical monocentric city model by Alonso et. al, which consists of multiple sectors and different income groups [26]. It consists of two industries and two household groups, where I_1 is an industry with low demand for horizontal space and high returns for agglomeration of human capital, for example, technology and consulting firms. The individuals who work in I_1 live in HH_1, household group 1, as they value a quick commute to work and have a low demand for land. Then, I_2 has a higher demand for land and employs the residents in HH_2. This could include industries like automotive or manufacturing firms. In 1b, we generalize HH_1 to be high-income and HH_2 to be low-income, as in the Kohl model, and we abstract the industries to be represented by nodes that are characterized into different destination types.

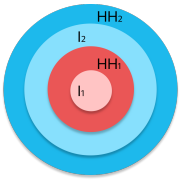

(a) HH_1: Income community number 1, HH_2: Income community number 2, I_1: Industry 1, where most of the population from HH_1 work and I_2: Industry 2, where most of the population from HH_2 work

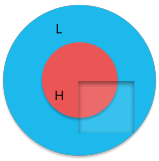

(b) H: high-income communities, L: low-income communities

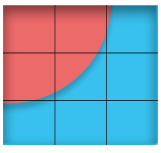

(c) Portion to analyze

Figure 1: Variation of the Kohl model based on distribution of incomes

[1] Bid-rent theory analyzes how demand and willingness to pay for land are a function of distance from the central business district (CBD).

2.1.1 Equations, Definitions and Parameters: Transportation Network Model

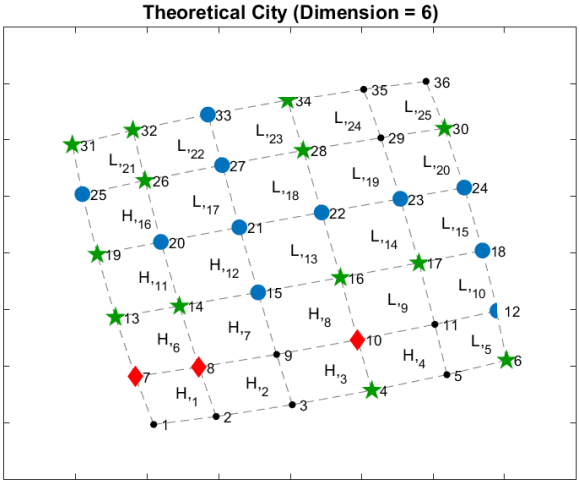

Figure 2: Theoretical City of dimension of 6. Blue circle: attractive to low-income; red diamond: attractive to high-income; green star: attractive to everyone; black: empty.

Node Type.

An individual node d_j represents a destination such as a job hub, health center, grocery store, shopping district, soup kitchen, park, etc. Not all destinations are attractive to every income group; they may only be attractive to a particular income group or none at all. Thus, we assign nodes to four broad categories, as seen in Figure 2: attractive to high-income, attractive to low-income, attractive to everyone. Equation (1) gives the node type of a node, d_j.

$$T(d_j) = \begin{cases} H, & \text{if node } j \text{ is attractive to high-income} \\ L, & \text{if node } j \text{ is attractive to low-income} \\ E, & \text{if node } j \text{ is attractive to everyone} \\ N, & \text{if node } j \text{ is empty} \end{cases} \tag{1}$$

Patch Type.

A face or patch represents a neighborhood which can be low-income, high-income, or non-residential, as in equation (2).

$$Q(A_i) = \begin{cases} H, & \text{if patch } i \text{ is high-income,} \\ L, & \text{if patch } i \text{ is low-income,} \\ N, & \text{if patch } i \text{ is non-residential.} \end{cases} \tag{2}$$

A particular neighborhood A_i has a constant population of individuals N_i. If $N_i = 0$, then the

face is a non-residential area. Otherwise, it is a low- or high-income neighborhood with population $N_i > 0$.

Attractiveness.

In considering the utility of a particular destination to various income groups, we define attractiveness to be the measure of how valuable a destination is to a particular income group. Therefore, the attractiveness of a node depends on the node type and patch type. Naturally, residents from high-income patches are attracted to H and E nodes, and disinterested in L and N nodes. Similarly, residents from low-income patches are attracted to L and E nodes, and impartial to H and N nodes. We quantify this through a function for attractiveness (3).

$$attr(Q(A_i), T(d_j)) = \begin{cases} \Lambda, & \text{if } T(d_j) = Q(A_i) = H. \\ \gamma, & \text{if } T(d_j) = Q(A_i) = L. \\ \sigma, & \text{if } T(d_j) = E \text{ and } Q(A_i) = H. \\ \nu, & \text{if } T(d_j) = E \text{ and } Q(A_i) = L. \\ 0, & \text{if } T(d_j) = L \text{ and } Q(A_i) = H, \\ & \quad \text{or } T(d_j) = H \text{ and } Q(A_i) = L, \\ & \quad \text{or } T(d_j) = N \text{ or } Q(A_i) = N. \end{cases} \tag{3}$$

Travel Time.

Each edge on the grid is of uniform distance. However, some edges represent bus routes. We define t_w to be the time it takes an individual from any patch to walk one edge, and t_b to be the time it takes an individual from any patch to ride the bus one edge. Thus, the time it takes an individual from patch A_i to travel from a node of patch A_i to node d_j is equal to $a*t_w+b*t_b$, where a is the number of edges walked and b is the number of edges traveled by bus. We are interested in finding the *fastest* path from a node in patch A_i to node d_j. The shortest path between A_i and d_j is defined to be the path with least travel time, which may not necessarily be unique and may include both walking and bus edges. Let $\Theta_{ij} = \{e_1, e_2, e_3, ...e_l\}$ where l is the number of directed edges in the shortest path from A_i to d_j and e_l is the last edge on the path, which contains node d_j. Then, accounting for the time it takes an individual to get from a location in their home patch to a home node, the travel time of the fastest path is $trt(A_i, d_j)$,

$$\text{trt}(A_i, d_j) = 0.25 + \sum_{e_k \in \Theta_{ij}} weight(e_k) \tag{4}$$

$$weight(e_k) = \begin{cases} t_b = 0.25, & \text{if } e_k \text{ is a bus route;} \\ t_w = 1, & \text{otherwise;} \end{cases} \tag{5}$$

Satisfaction.

We define *satisfaction* to be a measure of happiness with the public transportation system, or how easily residents can travel to the places attractive to their particular income group. The farther away a destination is from a patch, the less residents are willing to travel to it and the less it contributes to the patch's satisfaction. Thus, satisfaction is a function of attractiveness and travel time. Equation (6) is the satisfaction of a single patch over all the nodes in the grid.

$$Sat_{\text{patch}}(A_i) = \sum_{j=1}^{\text{TotalNodes}} \frac{attr(Q(A_i), T(d_j))}{trt(A_i, d_j)}. \tag{6}$$

We can raise the satisfaction of a patch by placing bus networks to shorten the travel time between the patch and the destinations attractive to their particular income group. Moreover, the overall satisfaction of the grid is the weighted sum of each patch in the grid multiplied by the fraction of the total population in the patch.

$$Sat_{\text{grid}} = \sum_{i=1}^{\text{TotalFaces}} \frac{N_i}{N_T} \cdot \text{Sat}_{\text{patch}}(A_i) \cdot W(A_i). \tag{7}$$

$$\text{where } W(A_i) = \begin{cases} w_{\text{low}}, & \text{if } Q(A_i) = L, \\ (1 - w_{\text{low}}), & \text{if } Q(A_i) = H. \end{cases} \tag{8}$$

w_{low} is the importance or weight given to the satisfaction of all low-income patches on the grid. Similarly, $(1 - w_{low})$ is the weight given to high-income patches. Hence, a value of $w_{low} = 0.5$ gives equal weight to the satisfaction of all income groups, while a value of $w_{low} = 0.2$ gives greater importance to the satisfaction of high-income patches. Equations (7) and (8) allow us to define the following optimization problem:

Maximize $\{\text{Potential bus routes}\}$	Sat_{grid}
subject to	Theoretical city with predetermined nodes and patches

It is to say, given a grid with predetermined node types and patch types, where a certain amount of edges can be bus routes, what layout of routes yields the highest Sat_{grid} for a given w_{low}? For the purposes of this paper, we will optimize the transportation networks for high-income

neighborhoods as well as for everybody. The results obtained from this optimization problem will allow us to model and analyze the epidemiological effects of transportation networks on low- and high-income groups during an outbreak of airborne disease.

Table 1: Variables in the transportation model

Notation	Definition
A_i	patch i
d_j	node k
$H = (\gamma, 0)$	attraction value of high-income node
$L = (0, \Lambda)$	attraction value of low-income node
$E = (\sigma, \nu)$	attraction value of everyone node
$N = (0,0)$	attraction value of empty node

Table 2: Parameters in the transportation model

Notation	Definition
N_i	population of patch i
N_T	total population
w_{low}	weight of low income patch in satisfaction optimization
$1 - w_{\text{low}}$	weight of high income patch in satisfaction optimization
t_w	amount of time it takes to travel one edge by walking
t_b	amount of time it takes to travel one edge by bus

Tables 1 and 2 list the variables and parameters used in the transportation network model. We will need to estimate many of these parameters for our simulations and sensitivity analysis.

2.1.2 Parameter Estimation: Theoretical Transportation Model

We estimate parameters for a lattice grid of 4 nodes by 4 nodes or, equivalently, 3 faces by faces. The grid is sufficiently large enough to model 81 mi^2, of an urban city while maintaining appropriate dimensions (9 mi^2) of faces to represent neighborhoods. We found that for a large city like New York City, NY, which has an area of approximately 308.9 mi^2, our grid is large enough to represent roughly a quarter of the total area. Using the 2010 census data for New York City as a guide, we let the total population of our lattice grid be 3,294,000 individuals.

We assume that it takes the average person 20 minutes to walk one mile, so that it takes an individual 60 minutes to travel one edge on the grid (3 mi). Similarly, we assume a bus traveling 30 mph takes 15 minutes (accounting for stops) to travel one edge. The transportation simulation uses a standard time unit of hours. Table 3 list values assigned to each node type for the simulations.

Table 3: Parameter estimates for the transportation model

Parameter	Value
γ	9
Λ	9
σ	5
ν	5
N_i	population of patch i
N_T	total population
w_{low}	weight of low income patch in satisfaction optimization
$1 - w_{low}$	weight of high income patch in satisfaction optimization
t_w	1 hour
t_b	0.25 hours

2.1.3 Optimization Methodology

To accomplish the objective of the first model, that is to find the optimal transportation network for the two cases, we need to know all the possible satisfaction values that a set of combinations of bus routes will give, and identify the set that maximizes the satisfaction. Case one is optimized for the high income, with $w_{low} = 0.2$; case two is optimized equally for both incomes, with $w_{low} = 0.5$.

The computational approach to this problem was made in MATLAB Software. This program allows the creation and processing of graph structures. For this, the dimension desired must be given to compute, which will indicate the total number of nodes (10), the total number of faces (9), and the total number of edges (11). For example, if the dimension is 2, then the structure will contain 1 face, 4 nodes and 4 edges. The second step is to identify the possible relationships between the nodes. This will allow the creation of the graph structure, including the set the incomes for the faces and the type for the nodes following the variation of the Kohl distribution.

Dimension, dim: number of nodes in a row/column.

$$\text{TotalFaces} = (dim - 1)^2 \tag{9}$$

$$\text{TotalNodes} = (dim)^2 \tag{10}$$

$$\text{TotalEdges} = 2 \cdot dim \cdot (dim - 1) \tag{11}$$

We index face A_i, node d_j, and edge e_k such that:

$i \in \{1, 2, ..., \text{TotalFaces}\}$

$j \in \{1, 2, ..., \text{TotalNodes}\}$

$k \in \{1, 2, ..., \text{TotalEdges}\}$

The next step is to identify all the possible sets of bus routes, when each edge in the grid is chosen to be a bus route or not. Thus to calculate every possible combination, we are essentially permuting a string of binary numbers that take into account the different localizations of the bus routes in the whole grid. For each set, we compute the satisfaction, and then we compare the satisfaction for all the sets, identify the maximum satisfaction and the current set related to it. Parallel processing is used to speed up the brute force optimization process, and each permutation will be calculate inside the parallel loop.

2.2 Multi-patch Influenza Epidemic Model

It is important to identify the role of the transportation system in the spread of an airborne disease. Therefore, a multi-patch SIR model is proposed to represent the epidemic spread of the Influenza A (H3N2) through the connections made by the transportation network. Influenza A is the respiratory infection virus and one of the main ways of its transmission is the airborne respiratory droplets. As mentioned above, the public transportation system like buses across the cities marks the continuous presence of this type of particles during the day. As a result, it is important to analyze the relation between the amount of time an individual spends on the bus and his chance of being affected by the disease while he was on the bus. To describe the population dynamics of this disease a SIR compartmental model is proposed, capturing the movement of individuals across the three stages of disease. To analyze the transition in each stage with respect to time, a system of differential equations were formulated that were parameterized by the proportion of time individuals spend on the public transportation system.

In order to build the model, it is important to identify the movement of people from one stage to another. A susceptible individual can become infected generally by the contact with an infected individual with a certain probability of effectiveness, known as the incidence rate. On the other stage, generally the infected can become recovered after a certain time. In order to define this model and especially the incidence rate, we use a similar approach as the one made by Castillo-Chavez, Song and Zhang [24]. This allows them to know the proportion of time spent on the subway, and off the subway. For this work, the mixing probabilities are based on the connections that a neighborhood, patch, can have with the other neighborhoods, patches, just by the transportation network, in other words, the only possible connection between patches is by a bus route. Additionally, the proportion of time spent on the bus system is determined by the satisfaction of the patch with the current transportation network.

2.2.1 Equations, Definitions and Parameters: Epidemic Model

As mentioned above, the multi-patch SIR compartmental model proposed is the next:

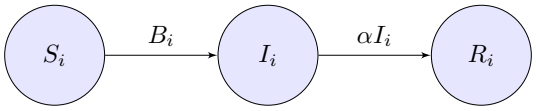

Figure 3: Flow diagram for SIR Model

The rate at which individuals from S progress to I is $B_i(t)$, the incidence rate, so that $\dot{S}_i(t) = -B_i(t)$. The rate at which individuals from I proceed to R is the recovery rate, α, thus $\dot{I}_i(t) = B_i(t) - \alpha I_i(t)$ and $\dot{R}_i = \alpha I_i(t)$. The total population of patch i at any time t is $N_i = S_i + I_i + R_i$. Note that N_i is constant for each patch. Individuals do not move between populations and no one is born into or dies in a population. To capture how individuals from various patches interact with one another within the multi-patch model, proportionate mixing probabilities are incorporated in $B_i(t)$.

$$\dot{S}_i = -B_i \tag{12}$$

$$\dot{I}_i = B_i - \alpha I_i \tag{13}$$

$$\dot{R}_i = \alpha I_i \tag{14}$$

$$B_i = \beta b_i S_i \left[\sum_{k=1}^{\text{TotalFaces}} \left(\overline{P}_{A_i A_k} \frac{I_k}{N_k} + P_{A_i A_k} \frac{I_k}{N_k} \right) \right] \tag{15}$$

The proportionate mixing probabilities account for all of the possible sources of infection for any given patch. They are defined as follows:

C_i is the set of patches connected to A_i by bus.

$$\overline{P}_{A_i A_k} = \begin{cases} \frac{b_k \tau_k N_k}{\sum_{m \in C_i} b_m \tau_m N_m} \tau_i, & \text{if } A_k \in C_i \\ 0, & \text{otherwise} \end{cases} \tag{16}$$

$$P_{A_i A_k} = \begin{cases} \frac{b_k \omega_k N_k}{\sum_{m \in C_i} b_m \omega_m N_m} \omega_i, & \text{if } A_k \in C_i \\ 0, & \text{otherwise} \end{cases} \tag{17}$$

Each probability represents the chance of the event that, given an individual from patch i makes a contact, this contact has happened *both* in a location *and* with an individual from patch k.

$$P(X \cap Y|Z) = P(\text{ event } X \ \cap \ \text{ event } Y \mid \text{event } Z)$$

where

$X =$ Contact takes place in location x,

$Y =$ Contact with individual from patch k

$Z =$ Individual from patch i makes a contact

We employ Bayes' Theorem in developing the probabilities. The probability $P(Y|B)$ in this case is the probability of event Y (contact occurring with individual from patch k) given event B, which is that, in location x, there are currently $x_k N_k$ people from patch k with contact rate b_k. For the construction of $b_k x_k N_k$, x_k can be either ω_k, the proportion of time spent on the bus system during the day, or τ_k, the proportion of time spend off the bus system during the day. Then, $b_k x_k N_k$ represents the average number of contacts that are caused by the average number of individuals from patch k in location x. We divide $b_k x_k N_k$ by the the total average number of contacts in location x with individuals from the remaining patches given that this kth patches can access to the actual one by the bus routes. $\overline{P}_{A_i A_k}$ and $P_{A_i A_k}$ represents the probability that given an individual from the i^{th} patch makes contact with an individual from the k^{th} patch off the bus and on the bus, respectively.

With interest in formulating a measure for average time spent on the bus, we define a modified shortest bus travel time, as seen in equation (18).

$$\text{trt}_B(A_i, d_j) = \sum_{e_k \in \Omega_{ij}} weight(e_k) \tag{18}$$

Here $\Omega_{ij} = \{e_1, e_2, ..., e_q\}$ is the set of edges in the shortest path between A_i and d_j (with cumulative least weight, not necessarily unique, bus edges only).

$q =$ the number of edges from A_i to d_j, e_q is an edge containing d_j.

Then, we can consider D_i to be the set of nodes that are connected to A_i by bus.

$$Sat_{B\text{patch}}(A_i) = \sum_{j \in D_i} \frac{attr(Q(A_i), T(d_j))}{trt_B(A_i, d_j)} \tag{19}$$

$$Sat_{B\text{node}}(A_i, d_j) = \frac{attr(Q(A_i), T(d_j))}{trt_B(A_i, d_j)} \quad \text{for} \quad j \in D_i \tag{20}$$

Equation (19) is used to calculate the overall satisfaction of a given patch. The satisfaction is a function of attraction and travel time. Here we are summing over the set of nodes connected to patch A_i by a bus route.

$$\rho_{ij} = \frac{Sat_{B\text{node}}(A_i, d_j)}{Sat_{B\text{patch}}(A_i)} \tag{21}$$

Equation (21) is used to calculate the probability that a path will be taken. The idea is that the satisfaction is the driving force behind an individuals decison to make a trip to a node. Therefore, we devide the satsifaction a patch recieves from a node over the overall satisfaction to get the probability.

$$\omega_i = \frac{2}{14} \sum_{j \in D_i} \rho_{ij} \cdot trt_B(A_i, d_j) \tag{22}$$

$$\tau_i = 1 - \omega_i \tag{23}$$

The above equation (22) calculates the proportion of time an individual spends on the bus. The total amount of time available for travel is 14 hours. An individual can make a round trip to any node they are connected to by a bus route. We sum the travel time to a node weighted by the probability of traveling to a node over the nodes a patch is connected to by bus. We multiply by 2 because we are considering round trips. Therefore, ω_i is the expected proportion of travel time in the bus routes in a day for the population of the ith patch, and τ_i is the expected proportion of time out the bus routes in a day.

The route an individual from A_i chooses to take can be thought of as a random variable. Consequently, the proportion of time the individual spends on the bus, ω_i, can be thought of as the expected value of travel time over the total amount of time available for travel. We call the total amount of time available for travel the active period and assume it to be 14 hours (24 hours minus 10 hours spent at home to rest). The expected travel time is the sum of the product of the time it takes to travel to each node $d_j \in D_i$ and the probability that the resident will travel to each node, ρ_{ij}. We assume all trips are round-trips in our formulation of ω_i and double the expected

travel time. Hence, the denominator of 7.

Table 4: Parameters in the SIR transportation model

Notation	Definition
b_i	per capita contact rate for residents from the i^{th} patch
β	transmission rate for residents from the i^{th} patch
α	recovery rate of the disease
ω_i	proportion of time residents from the i^{th} patch spend on the bus
$\tau_i = 1 - \omega_i$	proportion of time residents from the i^{th} patch spend off the bus
D_i	set of nodes connected to the i^{th} patch by bus route
C_i	set of patches connected to the i^{th} patch by bus route

With the exception of t_w and δ_i, all other parameters are recycled from the transportation model (See Tables 1 & 2).

2.2.2 Parameter Estimation: Epidemic Model

Four new parameters are introduced in the epidemic model: β, τ_i, ω_i, and b_i. We have defined ω_i and τ_i so that ω_i is the proportion of time residents from patch i spend on the bus and $\tau_i = 1 - \omega_i$ is the proportion of time residents from patch i spend off the bus.

The transmission probability β is assumed to be constant across patches, dependent on the disease. From past work on influenza modeling, we see typical β values to be in the range of 0.2 to 0.5. For example, in "Modeling the Impact of Behavior Changes on the Spread of Pandemic Influenza," the authors take β to be 0.4 [27]. In "Modeling Contact and Mobility Based Social Response to the Spreading of Infectious Diseases," $\beta = 0.2$ [27]. Thus, we choose $\beta \in \{0.2, 0.5\}$ for our estimates.

While transmission probability is assumed to be constant, the estimated patch contact rate b_i varies by patch type. It is assumed that all residents spend time within either households, workplaces, communities, or public transit at any given moment. In order to estimate contact rates by patch, we make use of a typical $\overline{\omega_i} = 0.047$, which can be interpreted as about 40 minutes per day spent on bus, as well as estimates from the American Time Use Survey [28] to give a weighted sum of contacts per day, using the following values considering workers from Cooley (2011) [29]:

Table 5: Mean contacts per day by location type

Location	Mean contacts per day
Household	0.922
Office	3.68
Subway	33.88
Community	34.80

Taking the average commute to be 40 minutes, the average time spent at home during the active period to be 2 hours, the average time spent at work to be 8 hours, and the average time spent in the community to be the remainder of the 14 hours, we can consider the weighted sum of the contact rates based on proportion of the active period of 14 hours.

Because the contact rate for the office estimated in [29] disproportionately considers smaller firms and does not account for about a million New York City jobs, we take it to represent the office contact rate for solely high-income individuals. Because many service jobs that are typically low-income require more interactions with individuals, for example in food service or janitorial and maid services, we consider the contact rate within the office for low-income individuals to be 10(Office) from Table 5. In our model, we take the contact rate for Subway in Table 5 to be equivalent to bus contact rate.

For $Q(A_i) = H$,

$$b_{i(H)} = \frac{2}{14}(\text{Household}) + \frac{8}{14}(\text{Office}) + \frac{2/3}{14}(\text{Subway}) + \frac{14-2-8-2/3}{14}(\text{Community})$$
$$b_{i(H)} = \frac{2}{14}(0.922) + \frac{8}{14}(3.68) + \frac{2/3}{14}(33.88) + \frac{10/3}{14}(34.80)$$
$$b_{i(H)} \approx 12.$$

For $Q(A_i) = L$,

$$b_{i(L)} = \frac{2}{14}(\text{Household}) + \frac{8}{14}(10)(\text{Office}) + \frac{2/3}{14}(\text{Subway}) + \frac{10/3}{14}(\text{Community})$$
$$b_{i(L)} = \frac{2}{14}(0.922) + \frac{8}{14}(10)(3.68) + \frac{2/3}{14}(33.88) + \frac{10/3}{14}(34.80)$$
$$b_{i(L)} \approx 31.$$

The average recovery rate α is estimated by considering the average recovery period with respect to the time units of our model. The average recovery period is one week. Thus, $\alpha = \frac{1}{7}$ days^{-1}

7	3	3,2	2	1	1
3	3	3,2	2	1	1
3	3	3,2	2	1	1
4	4	4,2	4,2	6,4,1	6,1
5,4	5,4	5,4	5,4	6,5,4	6
5	5	5	5	6,5	6

Figure 5: Example that shows the possible options for each patch

Table 6: Parameter estimates in the SIR transportation model

Parameter	Value
$b_{i(H)}$	12
$b_{i(L)}$	31
β	$\in \{0.2, 0.5\}$
α	$\frac{1}{7} \approx 0.1428$

2.2.3 Methodology and Simulations

We begin to explore the implications of this model by conducting analysis and simulation of the two-patch system. We place our epidemic model on top of a theoretical city generated from the former half of our work, to shed light on how transportation systems affect the spread of disease. There is greater emphasis placed on the parameters that vary across patches and by measures of satisfaction or transit access.

A given transportation network will generate interesting results in our model as it affects which patches interact with one another and which patches spend more or less time in the transit system. We can see below

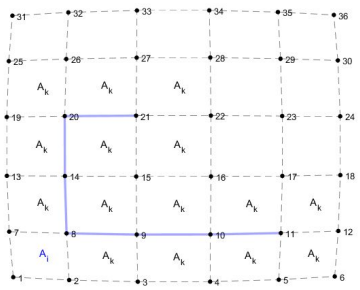

Figure 4: Example of the k_{th} patches connected to the i_{th} patch by a certain bus route

The darker edges on the above grid form a bus route. Given this bus route, the patches which are accessible to the patch labeled with i are itself and those labeled with k.

The above Figure 5 shows how the different networks can divide up the overall region into sub-regions when all of the network lines don't intersect. This is because the probabilities only allow mixing between connected patches. It is possible that patch i is connected to patch k and patch k is connected to patch m, but patch i is not connected to patch m. Figure 5 has 7 sub-regions. Notice how the top left face is isolated.

3 Analysis

We employ analytical techniques as well as numerical simulations to explore the dynamics and outcomes of our model. We begin by calculating the basic reproductive number, R_0, for both a single-patch and two-patch model. We explore the meaning of the basic reproductive number in the context of special cases. We employ sensitivity analysis on the basic reproductive number in order to determine which parameters have the largest impact on the epidemic.

The severity of the epidemic once it has ceased is measured by the final size equations. We derive final size relations as a system of equations for the two-patch model.

3.1 The Basic Reproductive Number

In seeking epidemic control strategies, one can investigate which parameters most affect the basic reproductive number, R_0. Then, investigate control startegies to change those parameters.

3.1.1 One-Patch System

In an effort to recognize pattern-forming as we increment to multi-patch models, we choose to begin by calculating the basic reproductive number for a one-patch model.
The equation is written below and for the derivation refer to the appendix.

$$R_0 = \frac{\beta b_1}{\alpha}$$

3.1.2 Two-Patch System

We consider a model with two patches connected by bus route.

For more simple notation, we define $\phi_{11} = \overline{P}_{A_1A_1} + P_{A_1A_1}$, $\phi_{12} = \overline{P}_{A_1A_2} + P_{A_1A_2}$, $\phi_{21} = \overline{P}_{A_2A_1} + P_{A_2A_1}$, and $\phi_{22} = \overline{P}_{A_2A_2} + P_{A_2A_2}$.

Also, define $R_{ij\tau} = \frac{\beta b_i}{\alpha}\overline{P}_{A_iA_j}$ and $R_{ij\omega} = \frac{\beta b_i}{\alpha}P_{A_iA_j}$

We conclude that

$$R_0 = \frac{(R_{11\tau} + R_{11\omega}) + (R_{22\tau} + R_{22\omega}) + \sqrt{((R_{11\tau} + R_{11\omega}) - (R_{22\tau} + R_{22\omega}))^2 + 4(R_{21\tau} + R_{21\omega})(R_{12\tau} + R_{12\omega})}}{2}$$

Again, for the derivation refer to the appendix.

$R_{ij\tau}$ represents the rate of secondary infections amongst residents of A_i by residents of A_j when individuals from both patches are off the bus. Conversely, $R_{ij\omega}$ represents the rate of secondary infections amongst residents of A_i by residents of A_j when individuals from both patches are on the bus. If $\omega_i = 0$,

$$R_0 = \tfrac{1}{2}[R_{11\tau} + (R_{22\tau} + R_{22\omega}) + \sqrt{(R_{11\tau} - (R_{22\tau} + R_{22\omega}))^2 + 4R_{21\tau}R_{12\tau}}]$$

Here R_0 is consistent with the meaning of $\omega_1 = 0$. The interpretation is that people from patch 1 do not ride the bus. Therefore, individuals from patch 1 can only make contact with an infected individual within their own patch, whether from patch 1 or patch 2. People from patch 2, however, are unrestricted; they can travel to patch 1. Therefore, people from patch 2 can become infected from contact with patch 2 individuals in their own patch, patch 2 individuals on the bus, and individuals from patch one or patch 2 while in patch 1. R_0 has a similar interpretation when ω_2 and not ω_1 is equal to zero. Now, consider $\tau_1 = 0$,

$$R_0 = \tfrac{1}{2}[R_{11\omega} + (R_{22\tau} + R_{22\omega}) + \sqrt{(R_{11\omega} - (R_{22\tau} + R_{22\omega}))^2 + 4R_{21\omega}R_{12\omega}}]$$

Here R_0 shows individuals from patch 1, who spend all of their time on public transportation, only come in contact with other individuals, whether from patch 1 or patch 2, while on the bus. R_0 also reflects the unrestricted movement of individuals from patch 2. Although individuals from patch 2 can travel to patch 1, no contact between patch 1 and patch 2 residents occurs off the public transportation system. Individuals from patch 2 can make contact with other individuals from patch 2 in any location. The explanation for $\tau_2 = 0$ is similar.

R_0 for a two-patch system does not hold when $\omega_1 = \omega_2 = 0$ or when $\tau_1 = \tau_2 = 0$. In the first scenario, we consider the patches to be isolated, their reproduction numbers are independent of each other. In the latter scenario, where both populations are entirely inside the public transportation system, two patches become one patch. In other words, the system can no longer be described by a multi-patch model.

Now, consider the following,
$\frac{1}{2}[(R_{11\tau}+R_{11\omega})+(R_{22\tau}+R_{22\omega})+\sqrt{((R_{11\tau}+R_{11\omega})-(R_{22\tau}+R_{22\omega}))^2}] \leq R_0 \leq \frac{1}{2}[(R_{11\tau}+R_{11\omega})+$
$(R_{22\tau}+R_{22\omega})+\sqrt{((R_{11\tau}+R_{11\omega})-(R_{22\tau}+R_{22\omega}))^2}+\sqrt{(R_{21\tau}+R_{21\omega})(R_{12\tau}+R_{12\omega})}]$

If $(R_{11\tau} + R_{11\omega}) < (R_{22\tau} + R_{22\omega})$. Then

$$(R_{22\tau} + R_{22\omega}) \leq R_0 \leq (R_{22\tau} + R_{22\omega}) + \sqrt{(R_{21\tau} + R_{21\omega})(R_{21\tau} + R_{21\omega})}$$

Similarly, if $(R_{22\tau} + R_{22\omega}) < (R_{11\tau} + R_{11\omega})$. Then

$$(R_{11\tau} + R_{11\omega}) \leq R_0 \leq (R_{11\tau} + R_{11\omega}) + \sqrt{(R_{21\tau} + R_{21\omega})(R_{12\tau} + R_{12\omega})}$$

Therefore,

$$max((R_{11\tau}+R_{11\omega}),(R_{22\tau}+R_{22\omega})) \leq R_0 \leq max((R_{11\tau}+R_{11\omega}),(R_{22\tau}+R_{22\omega}))+\sqrt{(R_{21\tau} + R_{21\omega})(R_{12\tau} + R_{12\omega})}$$

For a two-patch system, this means R_0 will be at least as large as the product of the rate of secondary infections amongst residents of A_i and A_i's internal mixing probabilities, $max((R_{11\tau} + R_{11\omega}), (R_{22\tau} + R_{22\omega}))$. Additionally, R_0 is at most the sum of $max((R_{11\tau} + R_{11\omega}), (R_{22\tau} + R_{22\omega}))$ and the geometric mean $\sqrt{(R_{21\tau} + R_{21\omega})(R_{21\tau} + R_{21\omega})}$. When we add $R_{ij\tau} = \frac{\beta b_i}{\alpha}\overline{P}_{A_iA_j}$ and $R_{ij\omega} = \frac{\beta b_i}{\alpha}P_{A_iA_j}$ we get $\frac{\beta b_i}{\alpha}(\overline{P}_{A_iA_j} + P_{A_iA_j})$ Since $\overline{P}_{A_iA_j}$ and $P_{A_iA_j}$ are the probability of mixing off and on the bus, respectively, they are disjoint and therefore when we add them we get the probability of mixing anywhere. Thus, here we are averaging the rate of secondary infections amongst residents of A_i by residents of A_j and the rate of secondary infections amongst residents of A_j by residents of A_i.

3.2 Formulation of Final Size Relations

Consider a two-patch system with total population of patch i being $N_i = S_i(t) + I_i(t) + R_i(t)$ and incidence rate of patch i being $B_i(t) = \beta b_i S_i[\Sigma_{k=1}^{n}(\overline{P}_{A_iA_k}\frac{I_k}{N_k} + P_{A_iA_k}\frac{I_k}{N_k})]$.

$$
\begin{aligned}
\dot{S_1} &= -\beta b_1 S_1\left[(\overline{P}_{A_1A_1} + P_{A_1A_1})\frac{I_1}{N_1} + (\overline{P}_{A_1A_2} + P_{A_1A_2})\frac{I_2}{N_2}\right] \\
\dot{I_1} &= \beta b_1 S_1\left[(\overline{P}_{A_1A_1} + P_{A_1A_1})\frac{I_1}{N_1} + (\overline{P}_{A_1A_2} + P_{A_1A_2})\frac{I_2}{N_2}\right] - \alpha I_1 \\
\dot{S_2} &= -\beta b_2 S_2\left[(\overline{P}_{A_2A_2} + P_{A_2A_2})\frac{I_2}{N_2} + (\overline{P}_{A_2A_1} + P_{A_2A_1})\frac{I_1}{N_1}\right] \\
\dot{I_2} &= \beta b_2 S_2\left[(\overline{P}_{A_2A_2} + P_{A_2A_2})\frac{I_2}{N_2} + (\overline{P}_{A_2A_1} + P_{A_2A_1})\frac{I_1}{N_1}\right] - \alpha I_2
\end{aligned}
$$

Note that the total population of both patches, N_1 and N_2 is constant.

In investigating these equations, we see:

$$(S_i + I_i)'(t) = -\alpha I_i \tag{24}$$

If $S_i \geq 0$ and $I_i \geq 0$, then $(S_i + I_i)(t)$ must be a smooth, non-negative, decreasing function, meaning it will go to a limit.

$$\lim_{t\to\infty}(S_i + I_i)(t) = S_{i\infty}, \text{ a constant.}$$

Taking the derivative of both sides,

$$\lim_{t\to\infty}(S_i + I_i)'(t) = 0$$

$$\therefore I_{i\infty} = \lim_{t\to\infty} I_i(t) = 0$$

At $t \to \infty$, there are no more infected individuals.

$N_i - S_{i\infty}$ is the final size of the epidemic in patch i, or the total number of unique infections in patch i over the course of the disease outbreak.

We calculated a system of equations which include $S_{1\infty}$ and $S_{2\infty}$ that can be solved by plugging in estimations for the other parameters. This can then be used to calculate the final sizes.

$$\ln\left(\frac{S_1(0)}{S_{1\infty}}\right) = (R_{11\tau} + R_{11\omega})\left(1 - \frac{S_{1\infty}}{N_1}\right) + (R_{12\tau} + R_{12\omega})\left(1 - \frac{S_{2\infty}}{N_2}\right) \tag{25}$$

$$\ln\left(\frac{S_2(0)}{S_{2\infty}}\right) = (R_{21\tau} + R_{21\omega})\left(1 - \frac{S_{1\infty}}{N_1}\right) + (R_{22\tau} + R_{22\omega})\left(1 - \frac{S_{2\infty}}{N_2}\right) \tag{26}$$

3.3 Sensitivity Analysis

In investigating the effects of various parameters, namely the bus time parameters ω_1 and ω_2, we can better understand the effects public transit has on the spread of disease. We employ sensitivity analysis of the basic reproductive number with respect to these parameters in order to understand their impact on the epidemic.

3.3.1 Sensitivity Indices for Two-Patch Basic Reproductive Number

In calculating the sensitivity indices for the basic reproductive number, we can begin by viewing it in terms of mixing probabilities as defined earlier:

$$R_0 = \frac{\beta b_1\phi_{11} + \beta b_2\phi_{22} + \sqrt{(\beta b_1\phi_{11} + \beta b_2\phi_{22})^2 - 4(\beta b_1\phi_{11}\beta b_2\phi_{22} - \beta b_2\phi_{21}\beta b_1\phi_{12})}}{2\alpha}$$

We explore the sensitivity of R_0 in relation to ω_1, ω_2, N_1, N_2, b_1 and b_2. The fact that ω_1 and ω_2 are directly controlled by the optimization network makes them good candidates for sensitivity analysis, as they vary by patch and are subject to change under different optimization constraints. Exploring the sensitivity of R_0 with respect to ω_1 and ω_2 will reveal the effects of disparate transit ridership on the spread of disease. We analyze the effect of N_1 and N_2 on R_0, because we can vary the geographic size of the patches to affect the population values. We also explore the effects of b_1 and b_2 on R_0, as the contact rates can be mitigated with cleaning strategies.

We discuss the process of deriving the sensitivity indices with respect to ω_1 and ω_2, while we guide the reader to the appendix in viewing the rest. The sensitivity index with respect to ω_1 is defined as the partial derivative of R_0 with respect to ω_1 normalized by multiplying by ω_1 over R_0.

When computing this partial derivative we get the partial derivatives of the ϕ_{ij}'s with respect to ω_1.

In order to explore the relationship between the parameters and the disease, we employ numerical simulation of the two-patch model along with sensitivity analysis. We consider change in parameters b_1, b_2, ω_1, ω_2, N_1, and N_2.

First, we will anlayze the sensitivity index of R_0 with respect to both b_1 and b_2, and investigate possible values in the range $b_i \in \{0, 100\}$. The two plots in Figure 6 show the sensitivity of R_0 at various values of b_1 and b_2.

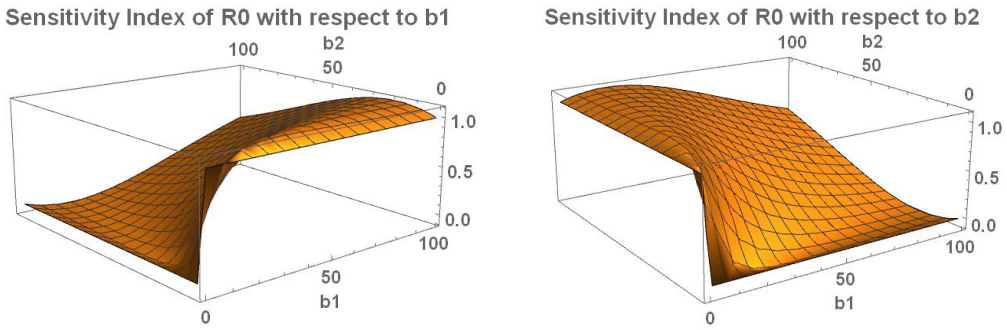

(a) (b)

Figure 6: Sensitivity indices for b_1 and b_2
($\beta = .015$, $n = 342000$, $\omega_1 = .01$, $\omega_2 = .01$, $\alpha = .143$)

Regardless of whether $b_i > b_j$ or $b_j > b_i$, R_0 has similar outcomes dependent on whether either value is large. From figure 6, in increasing either parameter R_0 will increase, and it will increase quicker at smaller values. Also, notice that the sensitivity index will always be larger when the parameter with which it is taken with respect to is the larger one.

The graphs in both figures 9 and 7 show the sensitivity indexes of R_0 at varying values of ω_1 and ω_2. These graphs are subject to the parameter estimations for the variables β, N_1, N_2, b_1, b_2, and α. The baseline values for these parameters are the following:

$$\beta = .2,\ N_1 = N_2 = 342000,\ b_1 = 13,\ b_2 = 32,\ \alpha = 0.143.$$

Note that here the N_1 and b_1 values reflect a high income patch while the N_2 and b_2 reflect a low income patch. With these values the above graphs have a few interesting characteristics. When describing these characteristics we will refer to the parameter the index is being taken with respect to as the main parameter and the other parameter as the secondary parameter.

First, notice that when the main parameter is zero the sensitivity index is zero. This makes sense because of the normalization to the index by multiplying by the parameter over R_0. Second, when holding the secondary parameter constant and increasing the main parameter the index

will increase. On the other hand, when holding the main parameter constant and increasing the secondary parameter the index will decrease. Finally, any change in the main parameter has a large impact on sensitivity index magnitude than the same change in the secondary parameter. Notice how when the main parameter is ω_2 the index can increase all the way to 1 while when ω_1 is the main parameter the index can only increase to just above 0.4. We believe this is because the per capita contact rate for patch 2 is so much larger than that of patch 1.

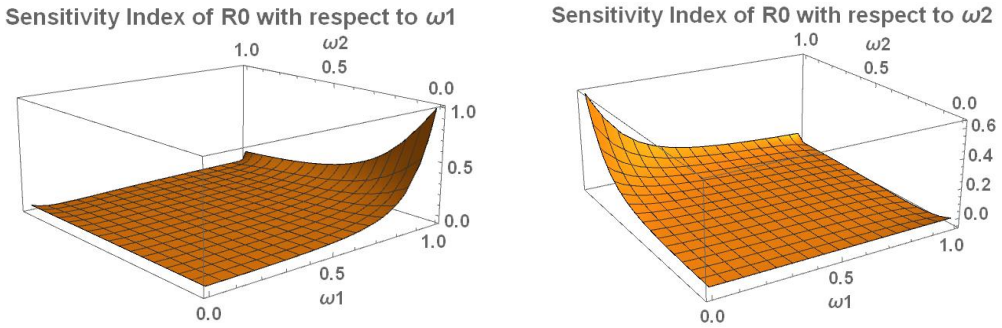

(a) (b)

Figure 7: $\beta = .015$, $n_1 = n_2 = 342000$, $b1 = 47$, $b2 = 30$, $\alpha = .143$

The plots above analyze the situation where the per capita contact rate of one patch is slightly larger than that of the other. Both indexes were larger when the parameter they were with respect to was closer to 1 and the other parameter was closer to 0. This was not affected by which contact rate was actually larger.

This can be understood because as one ω_i gets larger and the other gets smaller the populations begin to isolate themselves, one is always on the bus and the other in the patches. The individuals who make a lot of contact with others are sharing the same space and thus more transmissions occur than when people are evenly distributed based upon contact rate. This result can be illustrated with the simple numeric example that $47*47+30*30 = 3109$ contacts > 2820 contacts $= 47*30+47*30$. This does not happen when the parameter values are reversed and the parameter the indexes are with respect to approach 0 because of the normalization by the parameter.

The same can also be seen through the simulated results. We investigate the situation where $b_1 > b_2$ by testing different situations where $\omega_1 = \omega_2$ or where $\omega_1 > \omega_2$ by a great amount. Similar trends occur as in 9, but the magnitude of the effect that ω_i can have is lessened.

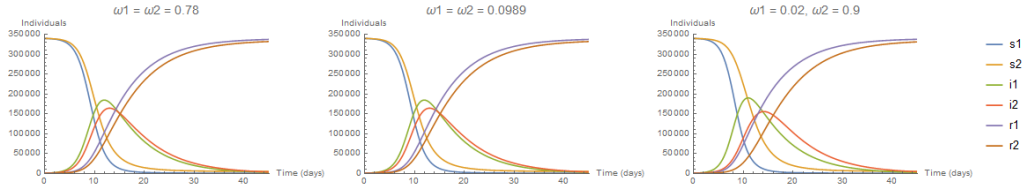

(a) (b) (c)

Figure 8: Investigating the relationship of ω_i values
($\beta = 0.015, b_1 = 65, b_2 = 41.3, \alpha = .143$)

Figure 8 showcases the effect that magnitude difference of the ω_i values can have on the epidemic outcome. The plots in (a) and (b) are striking because they exhibit the same behavior, while ω_i values are very different. In simulating many different combinations of ω_i values, it became clear that regardless of the values of ω_1 and ω_2, that if they are equal, they will have the minimum effect. Conversely, increasing their magnitude difference, irrespective of which belongs to the patch with higher b_i, results in more disparate epidemic results where the patch with greater b_i experiences the peak of the epidemic larger and sooner than the other patch. With ω_i values encroaching on each other, the disparity between the two patches' behavior decreases. This sheds more light on the sensitivity indices from 7, revealing that perhaps the patch-specific R_0 terms are changing quite a lot in magnitude but overall R_0 is only affected in the more extreme cases of ω_i values.

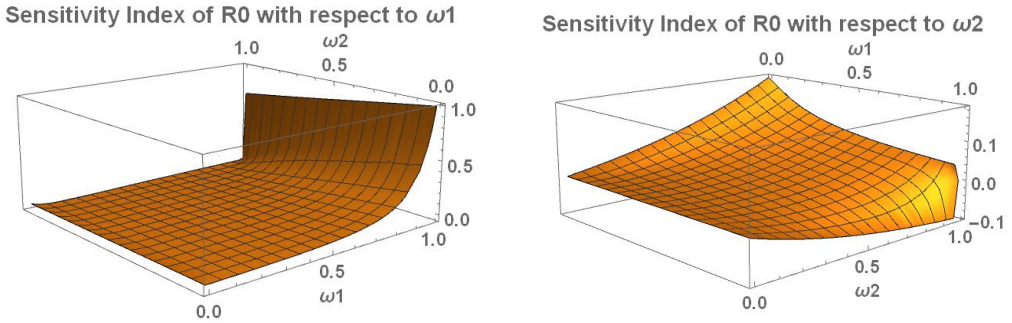

(a) (b)

Figure 9: $\beta = .015$, $N_i = 342000$, $b_1 = 70$, $b_2 = 13$, $\alpha = .143$

Figure 9 represents the sensitivity indices of R_0 with respect to ω_1 and ω_2 in the context of $b_1 > b_2$ by a large amount. In the case represented above, patch 1 has a higher contact rate and thus is more so the instigator of the disease. Increasing ω_1 will increase R_0, especially as it nears to 1, suggesting that the averaging effect within the R_0 is mostly controlled by patch 1 because of its higher contact rate, while the increase of ω_2 can lead to either a positive or negative sensitivity index depending on the respective ω_1. We can see that when ω_1 and ω_2 are very different, they tend to have larger-valued sensitivity indices but that when they are very similar they have a negligible value. For the sensitivity index of R_0 with respect to ω_1, different values of ω_2 do not

make a difference at smaller ω_1 and only play a slightly larger role at larger values of ω_1. These results can be clarified by interpreting the numerical solutions.

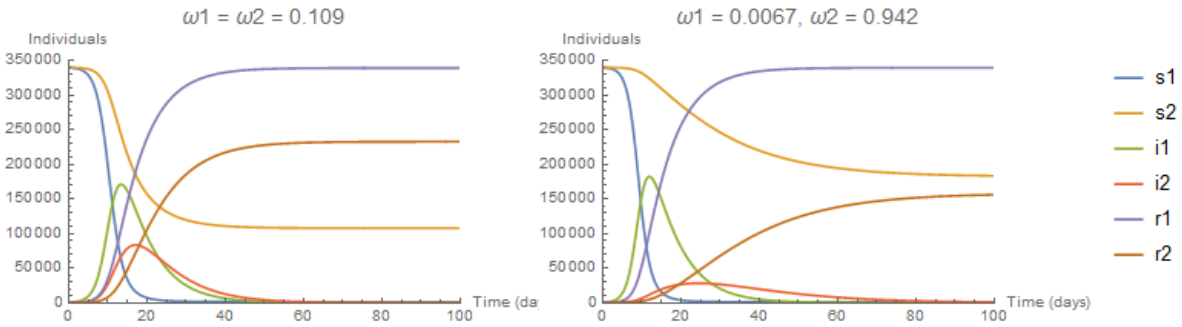

(a) (b)

Figure 10: The effect of magnitude difference in ω_i on the outcome of the epidemic
$\beta = .015$, $n_1 = n_2 = 342000$, $b1 = 58.3$, $b2 = 11.6$, $\alpha = .143$

It is again seen in Figure 10 that, in considering $b_1 > b_2$ with a larger difference, that ω_1 and ω_2 being closer in magnitude (as in 10(a)) results in each patch sharing a more similar epidemic process, when compared with plot (b) where ω_1 and ω_2 have very disparate values. The results are very similar to but lesser in magnitude than in Figure 9. The patch with the lower contact rate absorbs more of the epidemic when ω_i values are not disparate. In the contrary situation, patch 1 is hit by the epidemic much quicker and has a much larger final size of the epidemic compared to patch 2. This contextualizes the results for sensitivity analysis, in that the averaging of R_0 weakens the apparent effects of ω_i values, but when investigating on the patch level, it becomes clear that more disparate ω_i values cause more disparate epidemics between patches while similar ω_i values cause the epidemics to trend more similarly, in the presence of largely different contact rates by patch.

4 Results

4.1 Satisfaction within Transportation Networks

To examine the impact of limited transportation access on satisfaction, we consider grids in which only a quarter of the edges can be bus routes. Table 7 presents average total satisfaction of dimension-3 grids optimized for high-income neighborhoods and optimized for everybody.

Table 7: Average Satisfaction Values: 3x3 Grid

Optimization for	Average Sat_{grid}
High-income	0.484047
Everybody	0.713985

As seen in Table 8, the aforementioned trend persists in the dimension-4 grid.

Table 8: Average Satisfaction Values: 4x4 Grid

Optimization for	Average Sat_{grid}
High-income	0.712302
Everybody	0.853852

We found that, on average, the satisfaction of a city optimized for all income groups is about 0.23 points higher than a city optimized for only high-income groups. When bus routes are concentrated in high-income regions, low-income neighborhoods become isolated or disconnected from their places of interest. In other words, their satisfaction is much lower than the satisfaction of high-income neighborhoods, resulting in a low total-satisfaction for the entire community.

4.1.1 Transit Parameters Generated from the Transportation Networks

We use Equation (22) in order to generate ω_i values from the transportation networks. Table 9 shows the average ω_i values for high- and low-income neighborhoods based again on dimension-3 grids optimized for high-income neighborhoods or optimized for everybody.

Table 9: Average ω_i Values by Income Group: 3x3 Grid

Optimization for	ω_i for High-Income	ω_i for Low-Income
High-income	0.0092	0.0112
Everybody	0.0086	0.0124

We do the same for dimension-4 as seen in Table 10. As the grid grows larger, values are more comparable to what would be a realistic proportion of the 14-hour active period to spend in transit.

Table 10: Average ω_i Values by Income Group: 4x4 Grid

Optimization for	ω_i for High-Income	ω_i for Low-Income
High-income	0.0197	0.0116
Everybody	0.0173	0.0234

Table 11: Average satisfaction and ω_i values

w_{low} (Optimized for)	Average Sat_{grid}	ω_i for High-Income	ω_i for Low-Income
$w_{low} = 0.2$ (High-income)	0.712	0.0197	0.0116
$w_{low} = 0.5$ (Everybody)	0.854	0.0173	0.0234

The proportion of time high-income residents spend on the bus decreases on average when the public transportation network is optimized for everybody. In cases where the transportation routes are predominantly located in low-income areas, connected destinations contribute less to the satisfaction of high-income residents, resulting in lower proportions of time spent on public transit. On the other hand, when public transit is optimized for everyone, low-income residents spend a greater proportion of time on public transit, about 0.011 points more (Table 10). This means residents spend a greater amount of time on the bus if destinations connected by bus routes contribute to their satisfaction. Because we used the Kohl model to determine the placement of high and low-income areas, high-income neighborhoods are generally located near desirable destinations and low-income neighborhoods are situated farther away from desirable destinations. As a result, transportation networks have a greater effect on the ridership of low-income neighborhoods, as measured by the proportion of time spent on the bus, than on high-income neighborhoods.

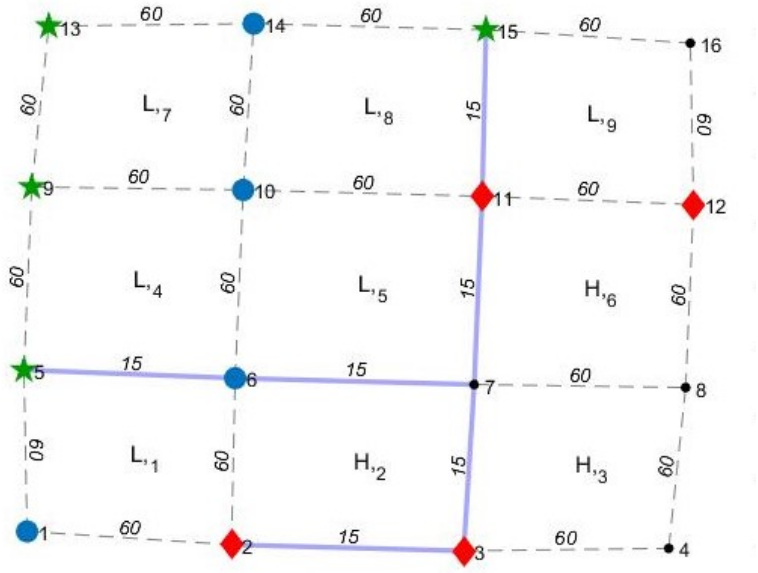

Figure 11: Transportation Network: Optimization for High-income (W_{low}=0.2)

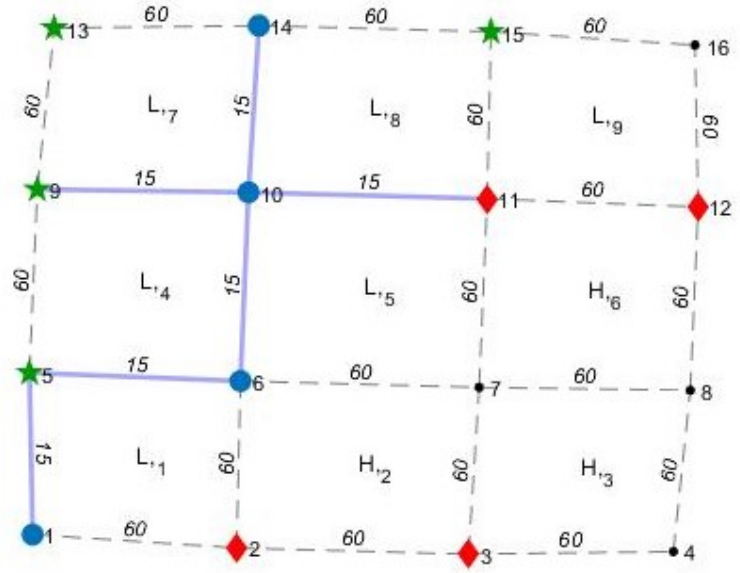

Figure 12: Transportation Network: Optimization for Everybody(W_{low}=0.5)

Figures 11 and 12 display the same grid but are optimized for different income groups. It is easy to see that by the layout of the Kohl model, low income groups, on average, have to travel farther to reach destinations of interest.

5 Discussion

Cities resembling the Kohl model may be heavily dependent on public transit systems. Modern cities seem to prioritize high-income neighborhoods when developing public transit systems. We examine what transportation systems look like when they are optimized for both high-income and low-income groups. By generating transportation systems under varied optimization schemes, we produce influential results. The data shows that overall satisfaction of our theoretical city is higher when transportation networks are designed to serve both income groups equitably. By equitably, we are referring to vertical "equity of opportunity," meaning that marginalized people should be identified and then given consideration in planning so they have adequate access to education and employment opportunities through the transportation system [13]. We do this by identifying low-income patches and setting our optimization weight to be 0.5. Because we use the Kohl model in distributing nodes and patches on our grid, it is given by default that low-income neighborhoods are less connected to desirable destinations. The more frequent placement of routes in low-income areas is a result of the optimization for everyone, and it produces the greatest increase in overall satisfaction when compared with placement in predominantly high-income areas. Our finding reinforces the common understanding within transportation equity literature that "accessibility-constrained people tend to gain relatively more from a given transportation improvement" [13]. Therefore, in optimizing for high-income neighborhoods and thus ignoring the needs of low-income neighborhoods, the overall satisfaction of the city suffers.

Ignoring the transit needs of low-income neighborhoods brings implications from the epidemic model. Using the data generated from the simulations as parameters, we came to interesting conclusions. Transportation networks optimized for high-income neighborhoods resulted in more disparity in ridership (measured by proportion of active period spent on bus) between the two income classes, compared with when optimizing for everyone. In other words, the average type-specific ω_i values generated by the transportation simulations were more disparate in optimizing for high-income groups when compared with ω_i values generated from the optimization for everyone. Sensitivity analysis on the basic reproduction number with respect to ω_1 and ω_2 showed that the relationship between ω_i values significantly affects the shapes of the patch-specific epidemics, while their contribution to the global basic reproductive number is relatively negligible when compared with contact rates. This makes sense in the context of the averaging property of our basic reproductive number.

The magnitude difference between ω_i values is what impacts the patch-specific epidemics. When the contact rates of patches are disparate, patches with low contact rates benefit from limited interaction with individuals with high contact rates, exhibiting a smaller final size and a smaller and later peak time. When decreasing the magnitude difference between ω_i values, the disparities

between the patches are lessened. While the intensity of the epidemic in the patch with the lower contact rate worsens as ω_i values are more equal, the implementation of cleaning and ventilation procedures to effectively lower contact rate while in transit would mitigate this effect. Equal mixing contributes to more equitable epidemic dynamics. Thus, the transportation networks that are optimized for everyone would generate transit parameters that result in less disparate epidemic outcomes when compared with the former. We can conclude that in making transit more accessible, useful, and desirable to all income groups, health disparities across the city are lessened.

The argument then becomes that we should optimize transportation networks for vertical equity, due to all the benefits of mass transit: sustainability, higher equity of opportunity, lower congestion, and a returns to scale that ensures the transportation system will have even more resources available to fund it. With increased ridership, transit systems will have more money available to them. Along with improved routes and service, transit systems must ensure that ventilation and cleanliness are prioritized. While the contact rates used in our implementation of the model were patch-specific averages based on previous literature, other works have employed differing contact rates while on or off the public transit systems. We acknowledge the role that transit can play in spread of disease, as we cited previous literature in the introduction. These were resulting from poor ventilation or cleanliness strategies, so we suggest that in investing money in lowering contact rates on subway, we can create more equitable transportation networks as well as mitigate health disparities across the city. Cleaning procedures on public transit should be implemented, as they may affect the total number of infections in a neighborhood. Then, we can heighten access to transportation and produce more equitable disease outcomes while not globally increasing the spread of disease.

In considering future work, we must point out some of the simplifications made in this report in order to to highlight the role of transportation networks in disease spread. For example, in the transportation model, we assumed attractiveness of destinations do not take negative values. Future work could incorporate the negative effects on satisfaction that being located near certain destinations may have, as is assumed in much of urban economics literature [8]. As for the mathematical model, future work should focus on sensitivity analysis of final size equations with respect to the ω_i parameter. We hope to incorporate more sophisticated residence times to keep track of the amount of time people spend in a given patch [30]. Simulation of more patches for the multi-patch model would generate new results to incorporate the concept from Figure 5. Analytically, exploring the basic reproductive number for a 3-patch system, while varying the transportation connectivity between the three patches, would allow unique insight into the dynamics of patches that are central places for mixing between many groups to occur. With ideas of "walkability" emerging in urban planning literature, we plan to incorporate walking time into transportation satisfaction, as well as multi-modal transit such as subway, commuter rail, and bus. Adding more

refined detail to nodes would consider the explicit inclusion of health centers, food centers, job centers, shopping districts, public amenities, and schools, in order to measure key forms of access. Likewise, future work could incorporate middle-income as well as mixed-income patches and demographic information of patches. In this way, we could make use of already-existing measures of access and utility within economics, such as the Gini coefficient or Shannon's diversity indices. In this way, we can allow the creation of transit networks that are more useful, accessible, and desirable to everyone.

6 Acknowledgements

We would like to thank the Mathematical and Theoretical Biology Institute (MTBI) co-Directors Dr. Carlos Castillo-Chavez, and Dr. Anuj Mubayi for giving us the opportunity to participate in this research program. We would also like to thank associate director Sherry Woodley, coordinator Ciera Duran and management intern Sabrina Avila for their efforts in providing logistics for activities during MTBI. We also want to give special thanks to Baltazar Espinosa, Dr. Benjamin Morin, Dr. Christopher Kribs, Dr. Carlos Castillo-Garsow, and Victor Moreno. These individuals helped us to accomplish our goals with guidance that went above and beyond what was expected, and we cannot emphasize enough the significance of their assistance. The research has been carried at the MTBI which is a Research Experience for Undergraduate (REU) summer program at the Simon A. Levin Mathematical, Computational and Modeling Sciences Center (SAL MCMSC) at Arizona State University (ASU). This project has been partially supported by grants from the National Science Foundation (DMS1263374), the National Security Agency (H98230-15-1-0021), the Office of the President of ASU, and the Office of the Provost at ASU.

References

[1] Zachary Neal. The Great Inversion and the Future of the American City, by Alan Ehrenhalt. *City & Community*, 12(3):280–282, 2013.

[2] Alan Ehrenhalt. The Great Inversion and the Future of the American City: EBSCOhost, 2014.

[3] Elizabeth Kneebone. The Growth and Spread of Concentrated Poverty, 2000 to 2008-2012.

[4] Adie Tomer, Elizabeth Kneebone, Robert Puentes, and Alan Berube. Missed Opportunity: Transit and Jobs in Metropolitan America, 2011.

[5] David Bruening. Transit Ridership Report. 1997.

[6] Matthew Dickens. Public Transportation Ridership Report. 2016.

[7] Todd Litman. Evaluating Public Transit Benefits and Costs. 2017.

[8] Edward L Glaeser, Matthew E Kahn, and Jordan Rappaport. Why Do The Poor Live In Cities? The Role of Public Transportation. 2017.

[9] Www.merriam-webster.com. Upward Mobility.

[10] Raj Chetty, Nathaniel Hendren, Patrick Kline, and Emmanuel Saez. Where is the land of opportunity? Intergenerational mobility in the US | VOX, CEPR's Policy Portal.

[11] The Burgess, Urban Land, and Use Model. The Burgess Urban Land Use Model. *Hofstra University*, pages 6–7, 2016.

[12] Raian Vargas Maretto, Talita Oliveira Assis, and Andre Augusto Gavlak. Simulating Urban Growth and Residential Segregation through Agent-Based Modeling. In *2010 Second Brazilian Workshop on Social Simulation*, pages 52–57. IEEE, oct 2010.

[13] Todd Litman. Evaluating Transportation Equity: Guidance for Incorporating Distributional Impacts in Transportation Planning. *Victoria Transport Policy Institute, Victoria, British ...*, 8(2):50–65, 2005.

[14] Zaheer Ahmad Nasir, Luiza Cintra Campos, Nicola Christie, and Ian Colbeck. Airborne biological hazards and urban transport infrastructure: current challenges and future directions. *Environmental science and pollution research international*, 23(15):15757–66, aug 2016.

[15] Airborne and Direct Contact Diseases - Infectious Disease Epidemiology Program - MeCDC; DHHS Maine.

[16] Arturo Casadevall and Liise-anne Pirofski. Microbiology: Ditch the term pathogen. *Nature*, 516(7530):165–166, dec 2014.

[17] C. B. Hall. The Spread of Influenza and Other Respiratory Viruses: Complexities and Conjectures. *Clinical Infectious Diseases*, 45(3):353–359, aug 2007.

[18] R. A. Weinstein, C. B. Bridges, M. J. Kuehnert, and C. B. Hall. Transmission of Influenza: Implications for Control in Health Care Settings. *Clinical Infectious Diseases*, 37(8):1094–1101, oct 2003.

[19] B Bean, B M Moore, B Sterner, L R Peterson, D N Gerding, and H H Balfour. Survival of influenza viruses on environmental surfaces. *The Journal of infectious diseases*, 146(1):47–51, jul 1982.

[20] Chris J Williams, Brunhilde Schweiger, Genia Diner, Frank Gerlach, Frank Haaman, Gérard Krause, Albert Nienhaus, Udo Buchholz, Andrew Hayward, and Jonathan Nguyen Van-Tam. Seasonal influenza risk in hospital healthcare workers is more strongly associated with household than occupational exposures: results from a prospective cohort study in Berlin, Germany, 2006/07. *BMC Infectious Diseases*, 10(1):8, dec 2010.

[21] Jason R. Andrews, Carl Morrow, and Robin Wood. Modeling the Role of Public Transportation in Sustaining Tuberculosis Transmission in South Africa. *American Journal of Epidemiology*, 177(6):556–561, mar 2013.

[22] Vulnerable groups. World Health Organization, 2016.

[23] Marsha L. Feske, Larry D. Teeter, James M. Musser, and Edward A. Graviss. Giving TB wheels: Public Transportation as a Risk Factor for Tuberculosis Transmission. *Tuberculosis*, 91:S16–S23, dec 2011.

[24] Carlos Castillo-Chavez, Baojun Song, and Juan Zhang. 8. An Epidemic Model with Virtual Mass Transportation: The Case of Smallpox in a Large City. In *Bioterrorism: Mathematical Modeling Applications in Homeland Security*, pages 173–197. Society for Industrial and Applied Mathematics, jan 2003.

[25] Lenee Blanton, Noreen Alabi, Desiree Mustaquim, Calli Taylor, Krista Kniss, Natalie Kramer, Alicia Budd, Shikha Garg, Charisse N. Cummings, Jessie Chung, Brendan Flannery, Alicia M. Fry, Wendy Sessions, Rebecca Garten, Xiyan Xu, Anwar Isa Abd Elal, Larisa Gubareva, John Barnes, Vivien Dugan, David E. Wentworth, Erin Burns, Jacqueline Katz, Daniel Jernigan, and Lynnette Brammer. Update: Influenza Activity in the United States During the 2016–17

Season and Composition of the 2017–18 Influenza Vaccine. *MMWR. Morbidity and Mortality Weekly Report*, 66(25):668–676, jun 2017.

[26] William Alonso. *Location and Land Use.* Harvard University Press, 1964.

[27] Piero Manfredi and Alberto D'Onofrio. *Modeling the Interplay Between Human Behavior and the Spread of Infectious Diseases.* Springer New York, New York, NY, 2013.

[28] Table 1. Time spent in primary activities and percent of the civilian population engaging in each activity, averages per day by sex, annual averages.

[29] Philip Cooley, Shawn Brown, James Cajka, Bernadette Chasteen, Laxminarayana Ganapathi, John Grefenstette, Craig R Hollingsworth, Bruce Y Lee, Burton Levine, William D Wheaton, and Diane K Wagener. The role of subway travel in an influenza epidemic: a New York City simulation. *Journal of urban health : bulletin of the New York Academy of Medicine*, 88(5):982–95, oct 2011.

[30] Victor Moreno, Baltazar Espinoza, Kamal Barley, Marlio Paredes, Derdei Bichara, Anuj Mubayi, and Carlos Castillo-Chavez. The role of mobility and health disparities on the transmission dynamics of Tuberculosis. *Theoretical Biology and Medical Modelling*, 14(1):3, dec 2017.

Appendix

A Robustness Check of Contact Probabilities

This work is to ensure that the sum of the contact probabilities is 1, as it should be when exhausting all possible options.

$$\begin{aligned}
\sum_{k=1}^{n}(\overline{P}_{A_iA_k} + P_{A_iA_k}) &= \sum_{k=1}^{n}\overline{P}_{A_iA_k} + \sum_{k=1}^{n}P_{A_iA_k} \\
&= \sum_{k\in C_i}\left[\frac{b_k\tau_kN_k}{\sum\limits_{m\in C_i}[b_m\tau_mN_m]}\tau_i\right] + \sum_{k\in C_i}\left[\frac{b_k\omega_kN_k}{\sum\limits_{m\in C_i}[b_m\omega_mN_m]}\omega_i\right] \\
&= \left(\frac{\sum\limits_{k\in C_i}[b_k\tau_kN_k]}{\sum\limits_{m\in C_i}[b_m\tau_mN_m]}\right)\tau_i + \left(\frac{\sum\limits_{k\in C_i}[b_k\omega_kN_k]}{\sum\limits_{m\in C_i}[b_m\omega_mN_m]}\right)\omega_i \\
&= \tau_i + \omega_i \\
&= 1
\end{aligned}$$

Therefore,

$$\sum_{k=1}^{n}(\overline{P}_{A_iA_k} + P_{A_iA_k}) = 1.$$

B Caclulating the Basic Reproductive Number

B.1 One-Patch System

$$\dot{S}_1 = -B_1$$
$$\dot{I}_1 = B_1 - \alpha I_1$$
$$\dot{R}_1 = \alpha I_1$$

Disease Free Equilibrium: $(S_1, I_1, R_1) = (N_1, 0, 0)$

$$F = B_1 \quad \frac{\partial F}{\partial I_1}|_{DFE} = \mathscr{F} = \beta b_1(\overline{P}_{A_1A_1} + P_{A_1A_1})$$

$$V = \alpha I_1 \quad \frac{\partial V}{\partial I_1}|_{DFE} = \mathscr{V} = \alpha \quad \mathscr{V}^{-1} = \frac{1}{\alpha}$$

Define $\phi_{11} = \overline{P}_{A_1A_1} + P_{A_1A_1}$. Then

$$\mathscr{F}\mathscr{V}^{-1} = R_0 = \frac{\beta b_1 \phi_{11}}{\alpha}$$

Note that in the case of a one patch system $\phi_{11} = 1$ and thus the $R_0 = \frac{\beta b_1}{\alpha}$.

B.2 Two-Patch System

$$\dot{S}_1 = -B_1$$
$$\dot{I}_1 = B_1 - \alpha I_1$$
$$\dot{R}_1 = \alpha I_1$$

$$\dot{S}_2 = -B_2$$
$$\dot{I}_2 = B_2 - \alpha I_2$$
$$\dot{R}_2 = \alpha I_2$$

Disease Free Equilibrium : $(S_1, I_1, R_1, S_2, I_2, R_2) = (N_1, 0, 0, N_2, 0, 0)$

$$F = \begin{pmatrix} B_1 \\ B_2 \end{pmatrix} \qquad \mathscr{J}(F)|_{DFE} = \mathscr{F} = \begin{pmatrix} \beta b_1(\overline{P}_{A_1A_1} + P_{A_1A_1}) & \frac{\beta b_1 N_1}{N_2}(\overline{P}_{A_1A_2} + P_{A_1A_2} \\ \frac{\beta b_2 N_2}{N_1}(\overline{P}_{A_2A_1} + P_{A_2A_1}) & \beta b_2(\overline{P}_{A_2A_2} + P_{A_2A_2}) \end{pmatrix}$$

$$V = \begin{pmatrix} \alpha I_1 \\ \alpha I_2 \end{pmatrix} \qquad \mathscr{J}(V)|_{DFE} = \mathscr{V} = \begin{pmatrix} \alpha & 0 \\ 0 & \alpha \end{pmatrix} \qquad \mathscr{V}^{-1} = \begin{pmatrix} \frac{1}{\alpha} & 0 \\ 0 & \frac{1}{\alpha} \end{pmatrix}$$

Define $\phi_{11} = \overline{P}_{A_1A_1} + P_{A_1A_1}$, $\phi_{12} = \overline{P}_{A_1A_2} + P_{A_1A_2}$, $\phi_{21} = \overline{P}_{A_2A_1} + P_{A_2A_1}$, and $\phi_{22} = \overline{P}_{A_2A_2} + P_{A_2A_2}$.

$$\mathscr{F}\mathscr{V}^{-1} = \begin{pmatrix} \frac{\beta b_1 \phi_{11}}{\alpha} & \frac{\beta b_1 N_1 \phi_{12}}{\alpha N_2} \\ \frac{\beta b_2 N_2 \phi_{21}}{\alpha N_1} & \frac{\beta b_2 \phi_{22}}{\alpha} \end{pmatrix}$$

Consider the characteristic equation

$$\begin{aligned} |\mathscr{F}\mathscr{V}^{-1} - \lambda| &= \begin{vmatrix} \frac{\beta b_1 \phi_{11}}{\alpha} - \lambda & \frac{\beta b_1 N_1 \phi_{12}}{\alpha N_2} \\ \frac{\beta b_2 N_2 \phi_{21}}{\alpha N_1} & \frac{\beta b_2 \phi_{22}}{\alpha} - \lambda \end{vmatrix} \\ &= (\frac{\beta b_1 \phi_{11}}{\alpha} - \lambda)(\frac{\beta b_2 \phi_{22}}{\alpha} - \lambda) - (\frac{\beta^2 b_2 \phi_{21} N_2 N_1 b_1 \phi_{12}}{\alpha^2 N_2 N_1}) \\ &= \frac{\beta^2 b_1 \phi_{11} b_2 \phi_{22}}{\alpha^2} - \lambda \frac{\beta b_1 \phi_{11}}{\alpha} - \lambda \frac{\beta b_2 \phi_{22}}{\alpha} - \frac{\beta^2 b_2 \phi_{21} b_1 \phi_{12}}{\alpha^2} + \lambda^2 \\ &= \lambda^2 - \lambda \frac{\beta b_1 \phi_{11} + \beta b_2 \phi_{22}}{\alpha} + \frac{\beta^2 b_1 \phi_{11} b_2 \phi_{22} - \beta^2 b_2 \phi_{21} b_1 \phi_{12}}{\alpha^2} \end{aligned}$$

The eigenvalues are as follows:

$$\lambda = \frac{\beta b_1 \phi_{11} + \beta b_2 \phi_{22} \pm \sqrt{(\beta b_1 \phi_{11} + \beta b_2 \phi_{22})^2 - 4(\beta b_1 \phi_{11} \beta b_2 \phi_{22} - \beta b_2 \phi_{21} \beta b_1 \phi_{12})}}{2\alpha}$$

Define $R_{ij\tau} = \frac{\beta b_i}{\alpha} \overline{P}_{A_i A_j}$ and $R_{ij\omega} = \frac{\beta b_i}{\alpha} P_{A_i A_j}$

$$R_0 = \frac{(R_{11\tau} + R_{11\omega}) + (R_{22\tau} + R_{22\omega})}{2}$$
$$+ \frac{\sqrt{((R_{11\tau} + R_{11\omega}) + (R_{22\tau} + R_{22\omega}))^2 - 4((R_{11\tau} + R_{11\omega})(R_{22\tau} + R_{22\omega}) - (R_{21\tau} + R_{21\omega})(R_{12\tau} + R_{12\omega}))}}{2}$$

This simplifies to:

$$R_0 = \frac{(R_{11\tau} + R_{11\omega}) + (R_{22\tau} + R_{22\omega}) + \sqrt{((R_{11\tau} + R_{11\omega}) - (R_{22\tau} + R_{22\omega}))^2 + 4(R_{21\tau} + R_{21\omega})(R_{12\tau} + R_{12\omega})}}{2}$$

C Final Size Equations

Consider a two-patch system with total population of patch i being $N_i = S_i(t) + I_i(t) + R_i(t)$ and incidence rate of patch i being $B_i(t) = \beta b_i S_i[\Sigma_{k=1}^{n}(\overline{P}_{A_iA_k}\frac{I_k}{N_k} + P_{A_iA_k}\frac{I_k}{N_k})]$.

$$\begin{aligned}
\dot{S_1} &= -\beta b_1 S_1 \left[(\overline{P}_{A_1A_1} + P_{A_1A_1})\frac{I_1}{N_1} + (\overline{P}_{A_1A_2} + P_{A_1A_2})\frac{I_2}{N_2}\right] \\
\dot{I_1} &= \beta b_1 S_1 \left[(\overline{P}_{A_1A_1} + P_{A_1A_1})\frac{I_1}{N_1} + (\overline{P}_{A_1A_2} + P_{A_1A_2})\frac{I_2}{N_2}\right] - \alpha I_1 \\
\dot{S_2} &= -\beta b_2 S_2 \left[(\overline{P}_{A_2A_2} + P_{A_2A_2})\frac{I_2}{N_2} + (\overline{P}_{A_2A_1} + P_{A_2A_1})\frac{I_1}{N_1}\right] \\
\dot{I_2} &= \beta b_2 S_2 \left[(\overline{P}_{A_2A_2} + P_{A_2A_2})\frac{I_2}{N_2} + (\overline{P}_{A_2A_1} + P_{A_2A_1})\frac{I_1}{N_1}\right] - \alpha I_2
\end{aligned}$$

Note that the total population of both patches, N_1 and N_2 is constant.

In investigating these equations, we see:

$$(S_i + I_i)'(t) = -\alpha I_i \tag{27}$$

If $S_i \geq 0$ and $I_i \geq 0$, then $(S_i + I_i)(t)$ must be a smooth, non-negative, decreasing function, meaning it will go to a limit.

$$\lim_{t\to\infty}(S_i + I_i)(t) = S_{i\infty}, \text{ a constant.}$$

Taking the derivative of both sides,

$$\lim_{t\to\infty}(S_i + I_i)'(t) = 0$$

$$\therefore I_{i\infty} = \lim_{t\to\infty} I_i(t) = 0$$

At $t \to \infty$, there are no more infected individuals.

$N_i - S_{i\infty}$ is the final size of the epidemic in patch i, or the total number of unique infections in patch i over the course of the disease outbreak.

We can integrate both sides of equation 27 for each patch for the entire time period, first for patch 1:

$$\int_0^\infty (S_1 + I_1)'(t)dt = -\alpha \int_0^\infty I_1 dt$$

By the fundamental theorem of calculus,

$$S_{1\infty} + I_{1\infty} - S_1(0) - I_1(0) = -\alpha \int_0^\infty I_1 dt$$

Because $I_{1\infty} = 0$ and $N_1 = S_1(0) + I_1(0)$,

$$\int_0^\infty I_1 dt = \frac{N_1 - S_{1\infty}}{\alpha}. \tag{28}$$

The same can be done for patch 2:

$$\int_0^\infty (S_2 + I_2)'(t) dt = -\alpha \int_0^\infty I_2 \, dt$$
$$S_{2\infty} + I_{2\infty} - S_2(0) - I_2(0) = -\alpha \int_0^\infty I_2 dt$$

$$\int_0^\infty I_2 dt = \frac{N_2 - S_{2\infty}}{\alpha}. \tag{29}$$

We can then take the equations for $\dot{S}_1$ and $\dot{S}_2$, divide by S_1 and S_2 respectively, and integrate:

First, for patch 1:

$$\int_0^\infty \frac{\dot{S}_1}{S_1} = \int_0^\infty -\beta b_1 \left[\left(P_{A_1 A_1} + \overline{P}_{A_1 A_1} \right) \frac{I_1}{N_1} + \left(P_{A_1 A_2} + \overline{P}_{A_1 A_2} \right) \frac{I_2}{N_2} \right] dt$$

Because N_1 and N_2 are constant with respect to time, they can be taken out of the integral along with all the other parameters.

$$\ln\left(\frac{S_1(0)}{S_{1\infty}}\right) = \frac{\beta b_1}{N_1} \left(P_{A_1 A_1} + \overline{P}_{A_1 A_1} \right) \int_0^\infty I_1 \, dt + \frac{\beta b_1}{N_2} \left(P_{A_1 A_2} + \overline{P}_{A_1 A_2} \right) \int_0^\infty I_2 \, dt$$

Substituting in equations 28 and 29 for $\int_0^\infty I_1 \, dt$ and $\int_0^\infty I_2 \, dt$, we result in a transcendental equation for $S_{1\infty}$ as a function of itself as well as $S_{2\infty}$ and parameters of interest.

$$\ln\left(\frac{S_1(0)}{S_{1\infty}}\right) = \frac{\beta b_1}{\alpha} \left(P_{A_1 A_1} + \overline{P}_{A_1 A_1} \right) \left(1 - \frac{S_{1\infty}}{N_1} \right) + \frac{\beta b_1}{\alpha} \left(P_{A_1 A_2} + \overline{P}_{A_1 A_2} \right) \left(1 - \frac{S_{2\infty}}{N_2} \right)$$

$$\ln\left(\frac{S_1(0)}{S_{1\infty}}\right) = (R_{11\tau} + R_{11\omega}) \left(1 - \frac{S_{1\infty}}{N_1} \right) + (R_{12\tau} + R_{12\omega}) \left(1 - \frac{S_{2\infty}}{N_2} \right) \tag{30}$$

We can mimic the process for patch 2 as follows:

$$\int_0^\infty \frac{\dot{S}_2}{S_2} = \int_0^\infty -\beta b_2 \left[\left(P_{A_2 A_1} + \overline{P}_{A_2 A_1} \right) \frac{I_1}{N_1} + \left(P_{A_2 A_2} + \overline{P}_{A_2 A_2} \right) \frac{I_2}{N_2} \right] dt$$

Then,

$$\ln\left(\frac{S_2(0)}{S_{2\infty}}\right) = \frac{\beta b_2}{N_2}\left(P_{A_2A_1} + \overline{P}_{A_2A_1}\right)\int_0^\infty I_1\ dt + \frac{\beta b_2}{N_2}\left(P_{A_2A_2} + \overline{P}_{A_2A_2}\right)\int_0^\infty I_2\ dt$$

Substituting in equations 28 and 29 for $\int_0^\infty I_1\ dt$ and $\int_0^\infty I_2\ dt$, we result in a transcendental equation for $S_{2\infty}$ as a function of itself as well as $S_{1\infty}$ and parameters of interest.

$$\ln\left(\frac{S_2(0)}{S_{2\infty}}\right) = \frac{\beta b_2}{\alpha}\left(P_{A_2A_1} + \overline{P}_{A_2A_1}\right)\left(1 - \frac{S_{1\infty}}{N_1}\right) + \frac{\beta b_2}{\alpha}\left(P_{A_2A_2} + \overline{P}_{A_2A_2}\right)\left(1 - \frac{S_{2\infty}}{N_2}\right)$$

$$\ln\left(\frac{S_2(0)}{S_{2\infty}}\right) = (R_{21\tau} + R_{21\omega})\left(1 - \frac{S_{1\infty}}{N_1}\right) + (R_{22\tau} + R_{22\omega})\left(1 - \frac{S_{2\infty}}{N_2}\right) \tag{31}$$

Equations 30 and 31 together describe the final size relations for the two-patch model.

D Sensitivity Indices

We define the partial derivatives as follows:

$$\frac{\partial \phi_{11}}{\partial \omega_1} = \sigma_{12} + 2\theta_{121}, \quad \frac{\partial \phi_{11}}{\partial \omega_2} = \epsilon_{12}, \quad \frac{\partial \phi_{12}}{\partial \omega_1} = \mu_{12} + \theta_{212}, \quad \frac{\partial \phi_{12}}{\partial \omega_2} = \psi_{21} + \theta_{211},$$

$$\frac{\partial \phi_{21}}{\partial \omega_1} = \psi_{12} + \theta_{122}, \quad \frac{\partial \phi_{21}}{\partial \omega_2} = \mu_{21} + \theta_{121}, \quad \frac{\partial \phi_{22}}{\partial \omega_1} = \epsilon_{21}, \quad \frac{\partial \phi_{22}}{\partial \omega_2} = \sigma_{21} + 2\theta_{212}$$

where we define ϵ_{ij},$\sigma_{ij}, \theta_{ijk}, \gamma_{ij},$ and ψ_{ij} to be:

$$\begin{aligned}
\epsilon_{ij} &= \frac{b_i b_j n_i n_j (1-\omega_i)^2}{(b_i n_i (1-\omega_i) + b_j n_j (1-\omega_j))^2} - \frac{b_i b_j n_i n_j \omega_i^2}{(b_i n_i \omega_i + b_j n_j \omega_j)^2} \\
\sigma_{ij} &= \frac{b_i^2 n_i^2 (1-\omega_i)^2}{(b_i n_i (1-\omega_i) + b_j n_j (1-\omega_j))^2} - \frac{b_i^2 n_i^2 \omega_i^2}{(b_i n_i \omega_i + b_j n_j \omega_j)^2} \\
\theta_{ijk} &= \frac{b_i n_i \omega_k}{b_i n_i \omega_i + b_j n_j \omega_j} - \frac{b_i n_i (1-\omega_k)}{b_i n_i (1-\omega_i) + b_j n_j (1-\omega_j)} \\
\gamma_{ij} &= \frac{b_i n_i \omega_i^2}{b_i n_i \omega_i + b_j n_j \omega_j} + \frac{b_i n_i (1-\omega_i)^2}{b_i n_i (1-\omega_i) + b_j n_j (1-\omega_j)} \\
\mu_{ij} &= \frac{b_i b_j n_i n_j (1-\omega_i)(1-\omega_j)}{(b_i n_i (1-\omega_i) + b_j n_j (1-\omega_j))^2} - \frac{b_i b_j n_i n_j \omega_i \omega_j}{(b_i n_i \omega_i + b_j n_j \omega_j)^2} \\
\psi_{ij} &= \frac{b_i^2 n_i^2 (1-\omega_i)(1-\omega_j)}{(b_i n_i (1-\omega_i) + b_j n_j (1-\omega_j))^2} - \frac{b_i^2 n_i^2 \omega_i \omega_j}{(b_i n_i \omega_i + b_j n_j \omega_j)^2}
\end{aligned}$$

Which, plugging in, and multiplying by $\frac{\omega_i}{r_0}$, results in equations for SI_{ω_1} and SI_{ω_2} as follows:

$$\begin{aligned}
SI_{\omega_1} &= \frac{\omega_1}{r_0}\frac{\partial r_0}{\partial \omega_1} \\
&= \frac{\omega_1}{2r_0}\left(\frac{b_2\beta\frac{\partial \phi_{22}}{\partial \omega_1} + b_1\beta\frac{\partial \phi_{11}}{\partial \omega_1} + 2(b_2\beta\frac{\partial \phi_{22}}{\partial \omega_1} + b_1\beta\frac{\partial \phi_{11}}{\partial \omega_1})(b_1\beta\gamma_{12} + b_2\beta\gamma_{21})}{\alpha}\right) \\
&\quad - \frac{4\left(b_1 b_2\beta^2\frac{\partial \phi_{22}}{\partial \omega_1}\gamma_{12} - b_1 b_2\beta^2\phi_{21}\frac{\partial \phi_{12}}{\partial \omega_1} - b_1 b_2\beta^2\frac{\partial \phi_{21}}{\partial \omega_1}\phi_{21} + b_1 b_2\beta^2\gamma_{21}\frac{\partial \phi_{11}}{\partial \omega_1}\right)}{\alpha^2} / \\
&\quad \left(2\sqrt{\left(\frac{b_1\beta\gamma_{12} + b_2\beta\gamma_{21}}{\alpha}\right)^2 - 4\left(\frac{b_1 b_2\beta^2\gamma_{12}\gamma_{21} - b_1 b_2\beta^2\phi_{21}\phi_{12}}{\alpha^2}\right)}\right) \qquad (32)
\end{aligned}$$

$$
\begin{aligned}
SI_{\omega_2} &= \frac{\omega_2}{r_0}\frac{\partial r_0}{\partial \omega_2} \\
&= \frac{\omega_2}{2r_0}\frac{\left(b_1\beta\frac{\partial\phi_{11}}{\partial\omega_2}+b_2\beta\frac{\partial\phi_{22}}{\partial\omega_2}\right)+2\left(b_1\beta\frac{\partial\phi_{11}}{\partial\omega_2}+b_2\beta\frac{\partial\phi_{22}}{\partial\omega_2}\right)(b_1\beta\gamma_{12}+b_2\beta\gamma_{21})}{\alpha} \\
&\quad -\frac{4\left(b_1b_2\beta^2\frac{\partial\phi_{11}}{\partial\omega_2}\gamma_{21}-b_1b_2\beta^2\phi_{21}\frac{\partial\phi_{21}}{\partial\omega_2}-b_1b_2\beta^2\frac{\partial\phi_{12}}{\partial\omega_2}\phi_{21}+b_1b_2\beta^2\gamma_{12}\frac{\partial\phi_{22}}{\partial\omega_2}\right)}{\alpha^2}/ \\
&\quad \left(2\sqrt{\left(\frac{b_1\beta\gamma_{12}+b_2\beta\gamma_{21}}{\alpha}\right)^2-4\left(\frac{b_1b_2\beta^2\gamma_{12}\gamma_{21}-b_1b_2\beta^2\phi_{21}\phi_{12}}{\alpha^2}\right)}\right)
\end{aligned}
\tag{33}
$$